solutions, the designated experiments met the requirements for conventional inversion-recovery ($T \gtrsim 4T_1$) for all carbons except the last one or two carbons of the side chain.)
(25) R. Freeman, H. D. W. Hill, and R. Kaptein, *J. Magn. Reson.*, 7, 327 (1972); S. J. Opella, D. J. Nelson, and O. Jardetzky, *J. Chem. Phys.*, **64**, 2533 (1976); R. K. Harris and R. H. Newman, *J. Magn. Reson.*, 24, 449 (1976).
(26) (a) T. M. Connor, *Trans. Faraday Soc.*, **60**, 1574 (1964); (b) J. Mikayke, *J. Polym. Sci.*, **28**, 477 (1958).
(27) K. S. Cole and R. H. Cole, *J. Chem. Phys.*, **9**, 341 (1944).
(28) J. Schaefer, *Macromolecules*, **6**, 882 (1973).
(29) (a) F. Heatley and A. Begum, *Polymer*, **17**, 399 (1976); (b) F. Heatley and M. K. Cox, *ibid.*, 18, 225 (1977).
(30) R. M. Fuoss and H. G. Kirkwood, *J. Am. Chem. Soc.*, **63**, 385 (1941).
(31) D. W. Davidson and R. H. Cole, *J. Chem. Phys.*, 18, 1417 (1950); **19**, 1484 (1951).
(32) F. Noack, "NMR Basic Principles and Progress", Vol. 3, Springer-Verlag, New York, N.Y., 1971.
(33) J. R. Macdonald, *J. Chem. Phys.*, **36**, 345 (1962).
(34) The present theory may also be inadequate to describe molecular dynamics in strongly aggregated low molecular weight compounds, such as 1,2-decanediol: G. C. Levy, M. P. Cordes, J. S. Lewis, and D. E. Axelson, *J. Am. Chem. Soc.*, **99**, 5492 (1977).
(35) P. L. Meyer, "Introductory Probability and Statistical Applications", Addison-Wesley, Reading, Mass., 1970.
(36) Y. K. Levine, *J. Magn. Reson.*, 11, 421 (1973).
(37) T. Yasukawa, D. Ghesquiere, and C. Chachaty, *Chem. Phys. Lett.*, **45**, 279 (1977).
(38) R. Deslauriers and R. L. Somorjai, *J. Am. Chem. Soc.*, 98, 1931 (1976).
(39) D. Doddrell and A. Allerhand, *J. Am. Chem. Soc.*, **93**, 1558 (1971).
(40) E. Breitmaier, K-H Spohn, and S. Berger, *Angew. Chem., Int. Ed. Engl.*, **14**, 144 (1975).
(41) N. J. M. Birdsall, A. G. Lee, Y. K. Levine, J. C. Metcalfe, P. Partington, and G. C. K. Roberts, *J. Chem. Soc., Chem. Commun.*, 757 (1973).
(42) (a) C. Chachaty, Z. Wolkowski, F. Piriou, and G. Lukacs, *J. Chem. Soc., Chem. Commun.*, 951 (1973); (b) J. Lyerla, Jr., H. M. McIntyre, and D. A. Torchia, *Macromolecules*, **7**, 11 (1974).
(43) K. Hatada, Y. Okamoto, K. Ohta, Y. Ymemura, and H. Yuki, *Makromol. Chem.*, **178**, 617 (1977).
(44) (a) J. C. Randall, *J. Polym. Sci., Polym. Phys. Ed.*, **14**, 1693 (1976); (b) J. R. Lyerla, T. T. Horikawa, and D. E. Johnson, *J. Am. Chem. Soc.*, **99**, 2463 (1977).
(45) A. Allerhand and R. K. Hailstone, *J. Chem. Phys.*, **56**, 3718 (1972).
(46) J. Schaefer and D. F. S. Natusch, *Macromolecules*, **5**, 416 (1972).
(47) Y. Inoue, A. Nishioka, and R. Chujo, *J. Polym. Sci., Polym. Phys. Ed.*, 11, 2237 (1973).
(48) J. D. Ferry, "Viscoelastic Properties of Polymers", Wiley, New York, N.Y., 1961; S. S. Rogers and L. Mandelkern, *J. Chem. Phys.*, **61**, 985 (1957).
(49) Preliminary data on a related polymer [poly(*n*-octyl acrylate)] indicate that ten bonds may be required in these polymers before relatively temperature independent NOEs are observed.
(50) M. P. N. Gent and J. H. Prestegard, *J. Magn. Reson.*, **25**, 243 (1977).
(51) Y. Inoue, T. Konno, R. Chujo, and A. Nishioka, *Makromol. Chem.*, **178**, 2131 (1977).

Cluster Model of Lipid Phase Transitions with Application to Passive Permeation of Molecules and Structure Relaxations in Lipid Bilayers

Minoru I. Kanehisa and Tian Yow Tsong*

Contribution from the Department of Physiological Chemistry, The Johns Hopkins University School of Medicine, Baltimore, Maryland 21205. *Received March 25, 1977*

Abstract: A phenomenological description of the gel to liquid-crystalline phase transition in lipid bilayers is presented in terms of Fisher's cluster model starting from the two-dimensional Ising model. A cluster is defined as a microdomain of lipid molecules in the nondominant phase linked together by nearest neighbors. The concept was inspired by many experimental observations suggesting the functional importance of the phase boundary during the lipid phase transition or phase separations of binary lipid mixtures. From the analysis of calorimetric data for phospholipid bilayers, it is concluded that the lipid membrane does not exhibit a strong cooperative transition from the complete gel phase to the complete liquid-crystalline phase. Instead, the lipid system contains a considerable amount of clusters of the nondominant phase, which may be of great biological importance. This aspect of bilayer behavior is well reflected on two kinds of experimental data: the passive permeation of molecules through the lipid membrane and the relaxation to a new equilibrium state after the temperature jump of liposome suspensions. By reviewing the experimental results on the phase transition dependence of the permeability of lipid bilayers, the permeation is classified basically into three types, corresponding to the permeation of water molecules, nonhydrophobic molecules, and hydrophobic molecules. The permeation of certain molecules, which has been reported to be enhanced appreciably at the midpoint of the gel to liquid-crystalline phase transition, is attributed to the "structurally disordered" boundary regions between two phases. The relaxation times obtained for the phase transition of lipid bilayers show a maximum at the transition temperature, which is also explained by a simple cluster reaction scheme.

I. Introduction

There have been a number of theoretical works on the cooperative transition in lipid membranes.[1-9] Most of them were mainly oriented to the elucidation of molecular mechanisms which cause the chain melting transition by the statistical mechanical treatments. We take a different approach by considering only the overall characteristics of the lipid system without knowledge of the precise nature of structural changes in each lipid molecule. The model is inspired by various experimental data which have recently become available concerning thermodynamics,[10] kinetics,[11] and certain functions of the lipid membrane.[12-19] Following Adam[20] we describe the properties of the lipid system by the two-dimensional Ising model. Similar treatments were once prevalent for the cooperative phenomena in biological membranes in relation to the nerve excitation.[20-22] However, in the nerve model the idea that the cooperative interactions between channels allow ion transport seems to have been replaced by the involvement of some carrier or pore molecules.[22] It should be noted here that our treatment is strictly confined to the uniform lipid system.

Experimental results have been presented on the phase transition dependence of several properties of the lipid membrane. The permeability of liposomes to certain ions or molecules, Na^+,[12] K^+,[13] ANS,[14] and Tempo-choline,[15] goes through a maximum with the rise of temperature at the midpoint of the lipid phase transition. The enhanced permeation was attributed to the boundary regions between solid and liquid domains and would possibly be explained by the structural defects[16] or the mismatch in molecular packing[15] at these in-

0002-7863/78/1500-0424$01.00/0

terfaces. Such observations are similar to the concept of lateral compressibility proposed by McConnell and co-workers.[17,18] They suggested that the coexistence of two lipid phases at the transition region of the pure lipid system or in the mixture of two lipid components would facilitate the transport and other biological functions of the membrane due to the high lateral compressibility or extensibility. In fact the hydrolysis of phospholipids by pancreatic phospholipase A_2 was strongly enhanced either near the phase transition temperature or by the phase separation of binary mixtures.[19] This concept was also confirmed in cell membranes. The activity of sugar transport systems in *E. coli* showed twofold discontinuities of the Arrhenius plots corresponding to the lateral phase separations of lipids.[17] It is probable that the phase changes of membrane lipids facilitate the conformational changes of membrane proteins; hence they play important roles in many biological functions.

We assume that there are at least three macroscopic states of the lipid membrane: the solidlike lipid domain, the fluidlike lipid domain, and the boundary between the two. The smaller domain, say a group of localized fluidlike structure within the dominant solidlike structure at lower temperature, is called the "cluster". The cluster is an old idea in the gas–liquid condensation phenomena.[23] Fisher[24] reviewed and extended the cluster model and applied this idea to the Ising system. Fisher's cluster model has been verified by computer experiments,[25] although there are many criticisms as well.[26] However, these discussions are from the point of view of the critical behavior which is too precise to be applicable for our use. Note that Fisher's model includes the importance of short-range forces in contrast to the mean field theory (Bragg–Williams approximation) which is equivalent to the infinite interaction range model.[27] Since it is more probable that the function of the lipid membrane is determined by the short-range order and it seems that the concept of the cluster has become popular,[11-19] we apply Fisher's cluster model to describe phenomenologically the lipid phase transition. The calorimetric data of the phase transition of phospholipid bilayers[10] are then analyzed in terms of the model. It is further shown that the model is particularly useful for the interpretation of passive diffusion of molecules through the lipid membrane and kinetic behavior around the phase transition region of lipid bilayers.

II. Cluster Model

The Ising model has been a popular tool as a "first approximation" to many biologically relevant phenomena. A helix–coil transition in linear biopolymers is one of the most successful applications of the one-dimensional Ising model.[28] Recently many types of protein denaturations were described in a unified manner by the Bragg–Williams approximation of the Ising model.[29] Similarly, as a first approximation, the lipid layer is considered as a two-dimensional Ising lattice. Each spin would correspond to one lipid molecule. We do not discuss the precise microscopic structure within the molecule, but expect that the molecule would exhibit one of only two distinguishable macroscopic conformational states after averaging over all possible configurations within the molecule. Namely, the first assumption is that the molecule takes either of two states, the solidlike S state or the fluidlike F state. Although the S state is well defined as the all *trans* configuration of the hydrocarbon chain, the F state is rather ambiguous and could be a mixture of many conformations containing at least one *gauche* configuration. We assume that the most probable or mean F state is characterized by the enthalpy gain ϵ over the S state. The possible number of configurations of the chain in the F state is incorporated as an entropy α. The second assumption concerns the cooperative interaction between molecules. We introduce the cooperativity as the clustering of molecules in the same state and denote the "surface tension" of the cluster by γ.

The cluster is defined as a microdomain of nondominant states. In our case it is a group of F states linked together by nearest neighbors below the chain melting temperature T_m and conversely it is a group of S states above T_m. The cluster is classified by the size l and the perimeter length s, that is, it is a group of l molecules in reverse state and has s molecules on the boundary between two states. If the cooperative energy γ is large enough and the temperature is lower than the critical temperature T_c, the cluster would take an almost circular shape and there would be few "defects" inside the cluster. Fisher assumed the most probable or mean perimeter length of the cluster of size l as[24]

$$\bar{s}(l) = s_0 l^{\sigma} \tag{1}$$

and incorporated the number of possible configurations as an entropy term. Here σ is one of two phenomenological exponents of Fisher's model and should be $\gtrsim 1/2$ in two dimensions. The partition function of an l-size cluster is

$$q_l = g(\bar{s}) u^l v_0^{\bar{s}} \tag{2}$$

where u and v_0 are defined as

$$u = \begin{cases} e^{-(\epsilon-\alpha T)/kT} & \text{below } T_m \\ e^{-(-\epsilon+\alpha T)/kT} & \text{above } T_m \end{cases} \tag{3}$$

$$v_0 = e^{-\gamma/kT} \tag{4}$$

Including the combinatorial factor $g(\bar{s})$, eq 2 can be rewritten as[24]

$$q_l = q_0 u^l v^{l^{\sigma}} / l^{\tau} \tag{5}$$

where $\tau \gtrsim 2$ is another phenomenological exponent of Fisher's model, and $l^{-\tau}$ has the same origin as the loop entropy of DNA,[28] i.e., the boundary line of a cluster must be closed to form a loop. The melting temperature T_m is defined from the bulk term u of eq 3

$$T_m = \epsilon/\alpha \tag{6}$$

The critical temperature T_c is defined from the surface term v

$$v = e^{-s_0(\gamma-\omega T)/kT} \tag{7}$$

as

$$T_c = \gamma/\omega \tag{8}$$

The surface entropy ω and the constant factor s_0 should be determined from the lattice structure. For the lipid system, however, it is better to leave $s_0\gamma$ and $s_0\omega$ as adjustable parameters.

If one neglects the interaction between clusters in the form of excluded volumes, the partition function Q of the system is given by[24]

$$\ln Q = \sum_l q_l \tag{9}$$

From this one can calculate several thermodynamic functions as follows:

(i) cluster distribution function

$$n_l = q_l = q_0 u^l v^{l^{\sigma}} / l^{\tau} \tag{10}$$

(ii) free energy

$$G = \begin{cases} G_+ - kT \sum_l n_l & \text{below } T_m \\ G_- - kT \sum_l n_l & \text{above } T_m \end{cases} \tag{11}$$

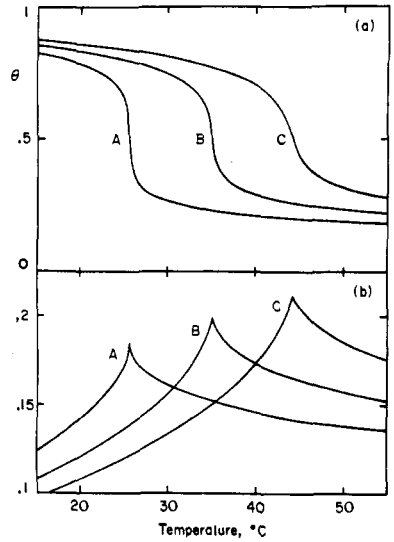

Figure 1. (a) The fraction of S states θ, eq 13, and (b) the amount of boundaries between S and F states η, eq 14, vs. temperature calculated for the lipid system by Fisher's cluster model with $l_{max} = 1000$. The critical temperature T_c is 35 °C, and the melting temperatures are A, $T_m = 25$ °C, $T_m' = 25.62$ °C; B, $T_m = T_m' = 35$ °C; and C, $T_m = 45$ °C, $T_m' = 44.20$ °C. The other parameters are $\epsilon = 1$ kcal/mol and $s_0\gamma = 1$ kcal/mol.

G_+: free energy of the complete S state structure

G_-: free energy of the complete F state structure

(iii) specific heat

$$C = \frac{1}{kT^2} \sum_l (\epsilon l + s_0\gamma l^\sigma)^2 n_l \tag{12}$$

(iv) fraction of S states (long-range order)

$$\theta = \begin{cases} 1 - \sum_l l n_l & \text{below } T_m \\ \sum_l l n_l & \text{above } T_m \end{cases} \tag{13}$$

(v) amount of boundaries between S and F states (short-range order)

$$\eta = \sum_l l^\sigma n_l \tag{14}$$

(vi) total number of clusters

$$\nu = \sum_l n_l \tag{15}$$

(vii) average cluster size

$$\xi = \sum_l l n_l \Big/ \sum_l n_l \tag{16}$$

The constants σ and τ are related to critical exponents.[24] From the exact solution for the planar Ising model, it is confirmed that $\sigma = 8/15$ and $\tau = 31/15$. We assume that at the critical point the relation $\theta(T_m = T_c) = 0.5$ holds for the lipid system, hence

$$q_0 = 0.5 \Big/ \sum_{l=1}^{\infty} l^{1-\tau} \tag{17}$$

The infinite series in eq 17 is convergent for $\tau > 2$ to give the Riemann function $\zeta(\tau - 1)$.

If the system size is finite, the summation in eq 9 and 11–17 is truncated at a certain value l_{max}. Note that the temperature T_m' where $\theta(T_m') = 0.5$ will be a little different from T_m defined by eq 6 in the finite system unless $T_m = T_c$. Therefore,

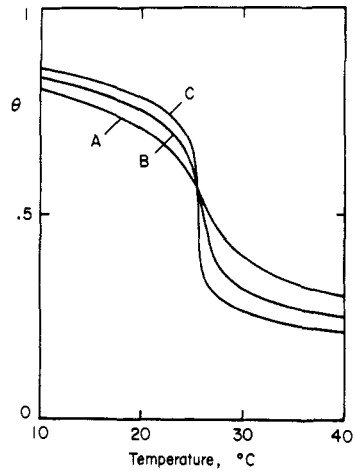

Figure 2. The effect of l_{max} on the order parameter θ of the lipid system calculated by Fisher's cluster model. A, $l_{max} = 100$; B, $l_{max} = 300$; and C, $l_{max} = 1000$, the same as the case A in Figure 1. The other parameters used are $\epsilon = 1$ kcal/mol, $s_0\gamma = 1$ kcal/mol, $T_c = 35$ °C, and $T_m = 25$ °C.

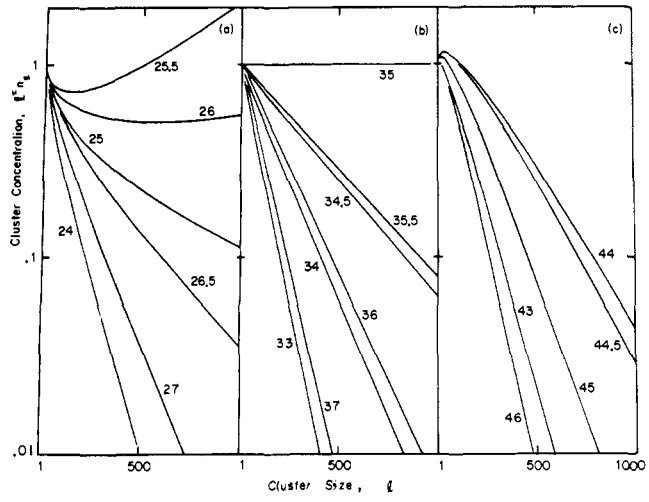

Figure 3. The cluster concentration $l^\tau n_l$, eq 10, vs. the cluster size l calculated by Fisher's cluster model at various temperatures. The cases of (a), (b), and (c) correspond to A, B, and C in Figure 1, respectively. The parameters used are $q_0 = 1$, $\epsilon = 1$ kcal/mol, $s_0\gamma = 1$ kcal/mol, $T_c = 35$ °C, and (a) $T_m = 25$ °C; (b) $T_m = 35$ °C; (c) $T_m = 45$ °C.

eq 3 must be redefined as

$$u = \begin{cases} e^{-(\epsilon - \alpha T)/kT} & \text{below } T_m' \\ e^{-(-\epsilon + \alpha T + 2\Delta)/kT} & \text{above } T_m' \end{cases} \tag{18a}$$

$$\Delta = \epsilon - \alpha T_m' \tag{18b}$$

so that the value of u coincides at T_m'. Equations 11 and 13 should also be changed accordingly. Figure 1 shows the result of the sample calculation of the cluster model with $l_{max} = 1000$. Three curves correspond to the cases of $T_m < T_c$, $T_m = T_c$, and $T_m > T_c$. The effect of the system size is given in Figure 2, where l_{max} is changed for the case of $T_m < T_c$. Figure 3 shows the cluster concentration n_l (multiplied by l^τ) at several temperatures for each case.

It is not easy to estimate the value of l_{max} from experimental data. Few people specify in their experiments the number of lipid molecules or the number of layers in one liposome and the distribution in size of their liposome preparations. The smallest single-bilayer lipid vesicle of 250 Å in diameter is known to contain about 2500 lipid molecules.[30] This vesicle shows a much broader transition curve than large multilamellar lipo-

somes, probably because of the large curvature which results in the small interaction energy between molecules. In the next section the experimental data are analyzed for unsonicated multilamellar liposomes which possibly contain 10^5–10^6 lipid molecules. Although the size and its distribution are not clear, one layer would contain more than 10^3 lipid molecules. We take the value of 1000 as the lowest estimate of l_{max}. The choice of larger l_{max} does not affect the result very much because the finite size effect is already small.

The critical temperature T_c has been estimated for monolayer lipids at the air–water interface from the surface pressure–area isotherm,[32] and T_c seems to be very close to the chain melting temperature T_m.[3,18] This being the case, the high temperature state of the lipid system is more like a mixing of S and F states. This can be compared with the case of $T_m \ll T_c$ or the very strong interaction energy, where the system undergoes the first-order phase transition from the complete S state structure to the complete F state structure. The analysis described below also suggests that the lipid system does not seem to exhibit a strong first-order phase transition and T_m would be very close to T_c.

III. Analysis of Equilibrium Experiments

The model contains five unknown parameters, l_{max}, ϵ, α (or T_m), $s_0\gamma$, and $s_0\omega$ (or T_c). We use the results of computer simulations for the simple two-dimensional Ising lattice as estimates of ω and s_0 for the lipid system. From exact enumerations for loops in two dimensions,[33] ω is estimated to be 2.83 eu for the plane triangular lattice. The value of s_0, although it is rather ambiguous, is around 3.4.[34] Hence, $s_0\omega$ is chosen to be 9.6 eu for the following discussion. Since the transition temperature T_m' is known from experimental data, the problem is to determine the values of three parameters, ϵ, $s_0\gamma$, and l_{max}. Before doing so it may be useful to derive an expression for the measure of cooperativity or the sharpness of the transition curve. The sharpness is measured in the finite system by the quantity

$$\frac{\partial\theta}{\partial(1/T)} = \frac{1}{k}\sum_{l=1}^{l_{max}} l(l + s_0\gamma l^{\sigma})n_l \tag{19}$$

at the transition temperature T_m'. For infinite l_{max} this corresponds to $u = 1$ and $T_m = T_m'$; hence eq 19 becomes

$$\left.\frac{\partial\theta}{\partial T}\right|_{T=T_m} = \frac{q_0}{kT_m^2}\sum_{l=1}^{\infty}(l^{2-\tau} + s_0\gamma l^{1+\sigma-\tau}) \times e^{-l^{\sigma}(s_0\gamma - s_0\omega T_m)/kT_m} \approx \frac{q_0}{\sigma T_m}\left(\frac{s_0\gamma}{kT_m}\right)^{(\tau-2)/\sigma} \times \Gamma\left(\frac{2-\tau+\sigma}{\sigma}\right)\left(1 - \frac{T_m}{T_c}\right)^{-(2-\tau+\sigma)/\sigma} \tag{20}$$

where Γ is the gamma function.

If one assumes that the lipid system undergoes a highly cooperative transition from complete S states to complete F states, the sharpness of the transition curve determines the van't Hoff enthalpy ΔH_{vH} in kcal/mol

$$\left.\frac{\partial\theta}{\partial T}\right|_{T=T_m} = \frac{\Delta H_{vH}}{RT_m^2} \tag{21}$$

The ratio of ΔH_{vH} to the actual enthalpy change per molecule ΔH_{cal} obtained calorimetrically is called the cooperative unit. It was used to determine the Zimm–Bragg parameter σ for linear polymers,[28] because the following relation holds.

$$\sigma^{-1/2} = \frac{\Delta H_{vH}}{\Delta H_{cal}} \tag{22}$$

This value also stands for the correlation length or the average length of helical sequences for an infinite chain with $\sigma \ll 1$ at the midpoint of the helix–coil transition. The actual value is usually estimated as 10–10^2 residues for long polyamino acids.

Table I. Transition Properties of Phospholipids in Multilamellar Aqueous Suspensions[10]

Lipid[53]	T_m, °C	ΔH_{cal}, kcal/mol	Cooperative unit, molecules
DMPC	23.9	5.4	330
DPPC	41.4	8.7	260
DSPC	54.9	10.6	130

Table II. Parameters of the Cluster Model for Phospholipids

Lipid[53]	l_{max}	ϵ^a	$s_0\gamma^a$	$u(T_m')$	$v(T_m')$	$\xi(T_m')$
DMPC	300	4.7	3.2	1.06	0.55	6.5
	500	4.5	3.0	1.02	0.78	4.8
	1000	4.4	2.9	1.01	0.92	4.3
DPPC	300	7.8	3.25	1.04	0.69	5.0
	500	7.7	3.1	1.01	0.88	4.2
	1000	7.6	3.05	1.00	0.95	4.1
DSPC	300	9.4	3.2	1.01	0.93	3.7
	500	9.4	3.15	1.00	1.00	3.6
	1000	9.4	3.1	0.99	1.08	3.5

[a] kcal/mol.

Unsonicated multilamellar phospholipid liposomes containing 10^5–10^6 lipid molecules are reported to have the cooperative unit of 10^2–10^3 molecules.[10] Although the apparent transition curve is much sharper than helix–coil transition curves as reflected on the values of the cooperative unit, care must be taken to interpret these values in the two-dimensional lipid system. The cooperative unit does not necessarily mean that the cluster of this size exists during the transition process. Note that the expression for the average cluster size is dependent on a model. In fact the cooperative unit of 10^2 for the system of 10^5 lipid molecules is better regarded as considerably low cooperativity (see below). For this purpose we estimate the correlation length in the cluster model or the average cluster size of eq 16 from experimental data.

In general photometric methods like light scatterings and absorption measurements, as well as such methods that use conformation-sensitive probes like fluorescence, ESR, and NMR, are dependent on the specific structures of lipid molecules and/or surrounding water molecules. On the other hand, calorimetric data reflect the nonspecific overall changes of the system and are suitable for analysis by our model. In Table I the transition properties obtained by Mabrey and Sturtevant[10] using high sensitivity scanning calorimetry are reproduced for three multilamellar phospholipids. Their data were used to determine the parameters ϵ and $s_0\gamma$ by adjusting the enthalpy of the system $H = \partial(G/T)/\partial(1/T)$ and the sharpness of the transition curve, eq 19, at T_m' with various values of l_{max}. Since the baseline of ΔH_{cal} is not known experimentally, the procedure of fitting $H(T_m') - H(0K)$ to $\frac{1}{2}\Delta H_{cal}$ was used. The result is shown in Table II. Although the value of l_{max} is not clear, it would be larger than 1000 as described before. The average cluster size would therefore be smaller than 5. However, this value should not be regarded as the "actual" cluster size. It must be remembered that this value is model dependent and that we have used Fisher's cluster model down to $l = 1$ cluster only for the sake of mathematical simplicity. In fact the term "cluster" should be attributed only to larger ones. The result of Table II only means that the lipid system does not exhibit strong cooperativity. This is because the critical temperature T_c is fairly close to the melting temperature T_m.[3,18] For example, $s_0\gamma$ = 3.2, 3.0, and 2.8 kcal/mol correspond to T_c = 60.2, 39.3, and 18.5 °C, respectively, if $s_0\omega$ = 9.6 eu. As can be seen in the table the value of v, which is to be compared with the Zimm–Bragg parameter $\sigma^{1/2}$, is fairly close to unity.

Table III. Permeability of Various Membranes to Water and Other Molecules

Membrane[53]	Water (osmotic)	K^+	Na^+	Cl^-	Ref
		Permeability Coefficient (cm/s)			
BLM (egg lecithin)	1.1×10^{-3}	3.4×10^{-12}	10^{-12}	$10^{-9} - 10^{-12}$	38
PS vesicle	4.4×10^{-3}	9.1×10^{-13}	1.6×10^{-13}	6.5×10^{-12}	40
Human erythrocyte	1.7×10^{-2}	2.4×10^{-10}	10^{-10}	2×10^{-4}	38,42
Squid axon (resting)	2.5×10^{-2}	5.6×10^{-7}	1.5×10^{-8}	1.0×10^{-8}	38
(excited)		17×10^{-5}	5×10^{-6}	10^{-8}	38
		Activation Energy (kcal/mol)			
PS vesicle	(8.25)[a]	30.4	27.0	13.6	40
Human erythrocyte	3.3	12-14	14-20	3-6	42

[a] A value for lecithin liposomes.[38]

In the next two sections we discuss the biological relevance of this result by analyzing passive permeation experiments and temperature jump experiments.

IV. Passive Permeation of Molecules

One of the most important advantages of the cluster model is that the phase boundary can be treated as the surface of the cluster. The possible significance of the phase boundary in mediating the penetration of molecules through the lipid membrane was first pointed out by Papahadjopoulos et al.[12] in the interpretation of their experimental results. They observed a maximum of the passive transport of Na^+ around the phase transition temperature of phospholipid vesicles, where the boundaries between gel and liquid-crystalline phases predominate. Since then similar observations have been reported for several other ions and molecules. The permeation was strongly enhanced around the lipid phase transition temperature.[12-15,18,35,36] Other substances showed either a discontinuity in the permeability or no significant change at the transition temperature.[14,37] According to the cluster model, a simplified picture on the passive transport is given. It is assumed that the permeation of a certain molecule occurs at three macroscopic states with different permeabilities depending on the physical and chemical nature of the molecule. Using the terminology of the model, the "ordered region" of the lipid system is defined as either the solidlike S state domain or the fluidlike F state domain. The "disordered region" represents the boundary between S and F state domains.

In general the permeability of lipid vesicles or bilayer lipid membranes (BLM) to water or ions is very low compared to that of actual cell membranes.[38-42] As shown in Table III, the permeability coefficient for the passive transport of small ions seems to be from 10^{-8} to 10^{-10} cm/s in cells, whereas it is around 10^{-12} cm/s in model systems. If one assumes that the small hydrophilic and amphiphilic molecules penetrate through the structurally disordered region of the membrane, this difference would reflect in part the amount of such disorders. The water permeability in lipid bilayers is fairly high as shown in Table III and not very different from that in cell membranes. One can speculate that the water molecules can penetrate the ordered region as well as the disordered region. They may be small enough to pass through the interstice between hydrophobic hydrocarbon chains. In fact the water permeation is higher above the transition temperature than below,[37,43] which is in accordance with the x-ray diffraction study showing the broadening of the lateral packing above the transition.[44] The water molecule may also penetrate faster through the larger interstice of the phase boundary. This was observed as a small peak of the water permeation at the phase transition temperature.[43]

The temperature dependence of the permeability determines the activation energy. The activation energy is usually correlated with the "pore size" and it becomes higher as the pore size becomes smaller. For the water permeation in liposomes, Blok et al.[37] obtained the values of 26 and 10 kcal/mol below and above the transition, respectively. Although these values may also contain the contribution from the change in the bilayer structure itself (see below), the apparent activation energy is higher for the better packed low-temperature state. Another interesting feature to note is the differenc in the activation energy between cells and model systems. As can be seen in Table III, it is always higher for lipid bilayers than cell membranes, which is consistent with the fact that the packing of molecules is better and closer in the uniform lipid system.

The permeability P of the lipid membrane is divided into three parts corresponding to three macroscopic states[12]

$$P(T) = P_s(T)\theta + P_f(T)(1 - \theta) + P_b(T)\eta \qquad (23)$$

where the subscripts s, f, and b stand for S state, F state, and boundary. The temperature dependence of each permeability is assumed to take the form

$$P_i(T) = P_i^0 e^{-E_i/RT} \qquad (i = \text{s, f, or b}) \qquad (24)$$

where P_i^0 is the temperature-independent part and E_i is the activation energy. The fraction of lipid molecules in the S state θ was defined by eq 13 and the amount of boundaries between S and F states η was defined by eq 14 as a sum of the perimeter length of clusters of all sizes. But here we retain the possibility that the boundary length η is to be correlated only with larger clusters, because the "physical cluster" which will produce enough structural disorders and allow the permeation on the boundary can be fairly large. Introducing the minimum size of the physical cluster l_{min}, the function η is redefined as

$$\eta = \sum_{l=l_{min}}^{l_{max}} l^{\sigma} n_l \qquad (25)$$

There have been several interesting observations of the relative permeability change during the lipid phase transition,[12-15,18,35-37] which are summarized in Table IV. In our most simplified treatment, these experiment are classified basically into three types.

(Type 1) Water molecules can penetrate through either of S, F, and B states, or else only through F and B states. The possible difference in the size of the interstice for each state leads to the assumption that $P_b > P_f > P_s$ and $E_b < E_f < E_s$.

(Type 2) Small ions and nonhydrophobic molecules can penetrate only through the largest interstice of B state; hence $P_f \approx 0$ and $P_s \approx 0$.

(Type 3) Small hydrophobic molecules, on the other hand, can penetrate only through the hydrophobic portion of S and F states; hence $P_b \approx 0$. It is also probable that $P_f > P_s$ and $E_f < E_s$.[14]

The result of model calculations for these three types of permeation is shown in Figure 4. Curves A and B represent

Table IV. Phase Transition Dependence of Molecular Permeation in Phospholipid Vesicles

Author	Lipid[53]	Molecule[53]	Observation	Type
Papahadjopoulos et al. (1973)	DPPG, DPPC	Na^+	Maximum	2
		Sucrose	Maximum	2
Wu and McConnell (1973)	DPPC	Valinomycin mediated K^+	Maximum	2
Inoue (1974)	DMPC, DPPC	Glucose	Enhancement[a]	2
Nicholls and Miller (1974)	DMPC, DPPC	K^+	Enhancement	2
		Cl^-	Enhancement	2
Blok et al. (1975)	DMPC, DPPC, +PA	K^+	Maximum	2
Tsong (1975)	DMPC, DPPC	ANS	Maximum	2
		BTB	Maximum	2
		Tetracycline	Break	3
		Chlortetracycline	Break	3
Marsh et al. (1976)	DMPC	Tempo-choline	Maximum	2
Blok et al. (1976)	DMPC, DPPC, +PA	Water	Jump	1

[a] The experimental data are available only for the lower half of the transition.

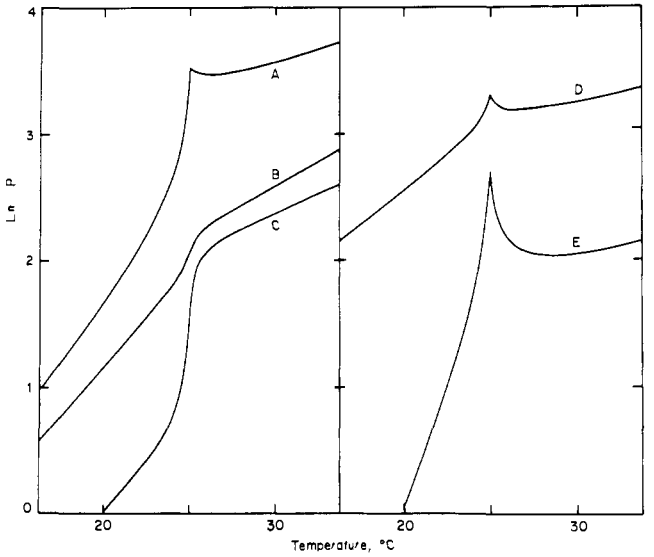

Figure 4. Three types of permeation according to the cluster model. A, typical type 1 permeation (water molecules) simulated with $P_s = 0$, $P_f(T_m'):P_b(T_m') = 1:15$, $E_f = 10$ kcal/mol, and $E_b = 5$ kcal/mol. B, typical type 3 permeation (hydrophobic molecules) simulated with $P_b = 0$, $P_f(T_m'):P_s(T_m') = 1:0.6$, $E_f = 10$ kcal/mol, and $E_s = 30$ kcal/mol. C, variation of type 1 or type 3 permeation where only P_f permeation is predominant, simulated with $P_s = P_b = 0$ and $E_f = 10$ kcal/mol. D, type 2 permeation for small nonhydrophobic molecules simulated with $l_{min} = 1$, $P_s = P_f = 0$, and $E_b = 8$ kcal/mol. E, type 2 permeation for larger nonhydrophobic molecules simulated with $l_{min} = 6$, $P_s = P_f = 0$, and $E_b = 25$ kcal/mol. The other parameters used are $\epsilon = 3$ kcal/mol, $s_0\gamma = 3$ kcal/mol, $s_0\omega = 9.6$ eu, $l_{max} = 300$, and $T_m' = 25$ °C. The logarithm of the permeability is given in an arbitrary unit.

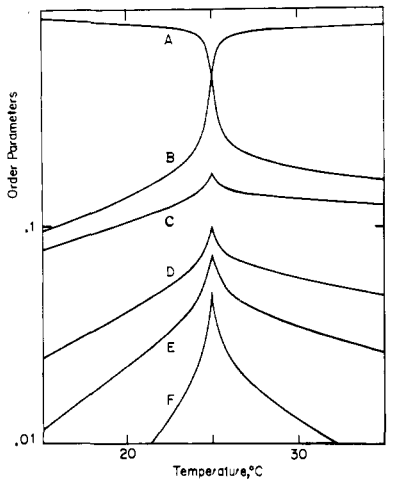

Figure 5. The order parameters of the lipid system plotted in the logarithmic scale vs. temperature calculated by the cluster model. A, θ; B, $1 - \theta$; C, η with $l_{min} = 1$; D, η with $l_{min} = 2$; E, η with $l_{min} = 3$; F, η with $l_{min} = 6$. The parameters used are $\epsilon = 3$ kcal/mol, $s_0\gamma = 3$ kcal/mol, $s_0\omega = 9.6$ eu, $l_{max} = 300$, and $T_m' = 25$ °C. The temperature dependence of these order parameters below and above the transition roughly corresponds to the activation energies of A, −0.80 and −2.6 kcal/mol; B, 6.2 and 0.54 kcal/mol; C, 4.8 and −1.3 kcal/mol; and E, 11 and −5.0 kcal/mol, respectively.

typical type 1 and type 3 permeation, respectively. The permeability for each state was chosen as $P_f(T_m'):P_b(T_m') = 1:15$ for curve A and $P_f(T_m'):P_s(T_m') = 1:0.6$ for curve B. The activation energies were assumed correspondingly, i.e., the larger value E_i for the smaller permeability $P_i(T_m')$. If P_b permeation is smaller for type 1 or if P_s permeation is smaller for type 3, both become more like curve C where only P_f permeation was assumed. Blok et al.[37] observed the water permeation similar to curve C by measuring the initial shrinkage velocity of liposomes after osmotic shocks. Tsong[43] also observed the small peak similar to curve A for the water permeation around the transition temperature, by following the turbidity change of DMPC and DPPC suspensions after the hypotonic shock in the stopped-flow apparatus. In the other experiments Tsong[14] obtained the type 3 permeation similar to curve B for hydrophobic tetracycline and chlortetracycline. Note that type 1 permeation was simulated in Figure 4 without incorporating the P_s term, although we do not exclude the possibility that the water permeation also occurs in the S state. But it is also possible that the lipid membrane has small F state defects well below the transition temperature due to the relatively low cooperativity and only these defects would permit permeation. The difference in the apparent activation energies below and above the transition can be accounted for by the temperature dependence of the functions $(1 - \theta)$ and η as shown in Figure 5.

For type 2 permeation two calculations are shown in Figure 4 as curves D and E, corresponding to smaller and larger nonhydrophobic molecules, respectively. The experiments show that the ANS transport is enhanced by 2–3 orders of magnitude at the midpoint of the transition,[14] while the change for Na^+ and K^+ is not very large.[12,13] A plausible explanation is that the larger ANS molecules require the larger interstice for permeation. This effect can be incorporated by discarding very small clusters assuming that their boundaries do not produce enough structural disorders. Hence, Figure 5 shows the result of η obtained by changing the minimum size of the physical cluster l_{min}. Note that the function η exhibits steeper temperature dependence as l_{min} is raised. Since the larger molecule requires the larger pore, the activation energy E_b should also

be larger. The large activation energy becomes the sharp decrease in η above the transition temperature, which results in a gradual increase in P, as shown in Figure 4, curve E. A more careful comparison of the ANS transport with the physical state of the lipid bilayer is given elsewhere.[14]

V. Kinetic Behavior

The other experimental evidence for the cluster model is found in the temperature jump relaxation kinetics of lipid bilayers.[11,45] The maximal relaxation time observed at the midpoint of the transition is a reflection of the slow nucleation process, that is, the formation of the cluster nucleus which is difficult to occur as a result of the cooperativity between molecules. A very simple cluster reaction scheme is described below so that the phase transition dependence of the kinetic behavior of lipid bilayers can be explained qualitatively by the cluster model.

We start from the single spin flip kinetic Ising model or Glauber model, where at most one lipid molecule undergoes the S $\rightleftarrows$ F transition in a unit time. Following Binder et al.[46] the dynamics of the total system are described in terms of the average cluster concentration

$$\bar{n}_l(t) = \langle n_l^\alpha(t)\rangle_\alpha \tag{26}$$

where α denotes symbolically the configuration of the cluster. If one neglects such spin flips as will result in the coalescence or the splitting off of clusters, the average cluster concentration is varied as

$$\frac{d\bar{n}_l(t)}{dt} = \langle n_{l-1}^\alpha(t) f_{l-1}^\alpha\rangle_\alpha - \langle n_l^\alpha(t) b_l^\alpha\rangle_\alpha - \langle n_l^\alpha(t) f_l^\alpha\rangle_\alpha + \langle n_{l+1}^\alpha(t) b_{l+1}^\alpha\rangle_\alpha \tag{27}$$

where f_l^α and b_l^α are the growth and shrinking rates, respectively, of the l-size cluster with configuration α.

If the distribution of many cluster configurations is sharply peaked at the most probable one, we take the factorization approximation,

$$\langle n_l^\alpha(t) f_l^\alpha\rangle_\alpha \approx \langle n_l^\alpha(t)\rangle_\alpha \langle f_l^\alpha\rangle_\alpha \equiv \bar{n}_l(t)\bar{f}_l \tag{28a}$$

$$\langle n_l^\alpha(t) b_l^\alpha\rangle_\alpha \approx \langle n_l^\alpha(t)\rangle_\alpha \langle b_l^\alpha\rangle_\alpha \equiv \bar{n}_l(t)\bar{b}_l \tag{28b}$$

Thus, eq 27 is written

$$\frac{d\bar{n}_l(t)}{dt} = \bar{f}_{l-1}\bar{n}_{l-1}(t) - (\bar{f}_l + \bar{b}_l)\bar{n}_l(t) + \bar{b}_{l+1}\bar{n}_{l+1}(t) \tag{29}$$

This is equivalent to the simple kinetic scheme

$$\ldots \rightleftarrows l-1 \underset{\bar{b}_l}{\overset{\bar{f}_{l-1}}{\rightleftarrows}} l \underset{\bar{b}_{l+1}}{\overset{\bar{f}_l}{\rightleftarrows}} l+1 \rightleftarrows \ldots \tag{30}$$

where each cluster grows and shrinks step by step with effective rate constants $\bar{f}_l$ and $\bar{b}_l$. In our problem the boundary conditions are $\bar{n}_1(t) \equiv 0$ and $\bar{n}_{l_{max}+1}(t) \equiv 0$.

We further assume that the reaction occurs only on the boundary of the cluster due to the cooperativity between molecules. If the reaction rate does not depend on the curvature of the cluster boundary, in other words, if the difference in the number of nearest neighbors in the opposite state is not considered, the reaction rate is proportional to the boundary length l^σ, hence the average cluster growth/shrinking rate takes the form

$$\bar{f}_l = \bar{f} l^\sigma \qquad (l \geq 1) \tag{31a}$$

$$\bar{b}_l = \bar{b} l^\sigma \qquad (l \geq 1) \tag{31b}$$

The rate for the nucleation process or the formation of a size-one cluster is denoted by $\bar{f}_0$. These rate constants are determined from the detailed balance condition at equilibrium,

$$\bar{f}_l \bar{n}_l(\infty) = \bar{b}_{l+1}\bar{n}_{l+1}(\infty) \qquad (l \geq 0) \tag{32}$$

except one elementary rate constant $\bar{b}$. The equilibrium cluster concentration $\bar{n}_l(\infty)$ is given by eq 10.

In terms of the eigenfunction expansion, the solution of eq 29 can be represented as

$$\bar{n}_l(t) = \bar{n}_l(\infty) + \sum_{j=1}^{l_{max}} c_l^j e^{-\lambda_j t} \tag{33}$$

The eigenvalues λ_j are easily obtained by the direct diagonalization of the tridiagonal matrix A,[47]

$$A = \begin{bmatrix} -\bar{f}_0 & \bar{b}_1 & & & \\ \bar{f}_0 - (\bar{b}_1 + \bar{f}_1)\bar{b}_2 & & & & \\ & \bar{f}_1 & -(\bar{b}_2 + \bar{f}_2)\bar{b}_3 & & \\ & & \cdots\cdots\cdots\cdots & & \\ & & & \bar{f}_{l_{max}-2} - (\bar{b}_{l_{max}-1} + \bar{f}_{l_{max}-1})\bar{b}_{l_{max}} & \\ & & & \bar{f}_{l_{max}-1} & -\bar{b}_{l_{max}} \end{bmatrix} \tag{34}$$

The amplitudes c_l^j are determined from the corresponding eigenvectors and the initial concentration $\bar{n}_l(0)$.[48]

Our concern is the relaxation of the order parameter θ, so that

$$\theta(t) - \theta(\infty) = \sum_{j=1}^{l_{max}} \alpha_j e^{-t/\tau_j} \tag{35}$$

where

$$\tau_j = 1/\lambda_j \tag{36}$$

$$\alpha_j = \sum_{l=1}^{l_{max}} l c_l^j \tag{37}$$

As a model calculation, the relaxation times are plotted in Figure 6 vs. temperature using the same parameters as those for Figures 4 and 5, and with the elementary rate constant $\bar{b} = 1$. The maximal relaxation time is observed at the midpoint of the transition, which is most prominent for the slowest relaxation τ_1. The enhancement is nearly three orders of magnitude. In order to see how appreciably each relaxation process is detected, one has to calculate the relaxation amplitudes. The amplitudes for temperature jumps from the complete S state structure ($\theta = 1$) is shown in Figure 7, where we used the smaller value of $l_{max} = 50$. As the transition temperature becomes closer, the largest relaxation time which reflects the nucleation process becomes more and more predominant.

We have reported the experimental results on the temperature jumps of DMPC and DPPC suspensions and obtained two relaxation times for the gel to liquid-crystalline phase transition.[11] The slower relaxation time or the final slope of the experimental relaxation curve can be approximated by the largest relaxation time τ_1 in this model. On the other hand, the faster one may be related to the initial slope or the Schwarz mean relaxation time τ^*,[49]

$$\frac{1}{\tau^*} = \sum \frac{\alpha_j}{\tau_j} \Big/ \sum \alpha_j \tag{38}$$

although τ^* should be considered as the lower bound. If one compares these two relaxation times with the experiments, the following qualitative features are consistent. Both relaxation times show a maximum at the transition temperature T_m and also the amplitude for the slower process reaches a maximum around T_m.[50] Experimentally the τ–T curve is not symmetric and the gradual increase in τ with decreasing temperature is observed below the transition region. This can be explained by incorporating the temperature dependence of the elementary rate constant $\bar{b}$ in the form of $\bar{b} \propto e^{-E/RT}$, where E is the Ar-

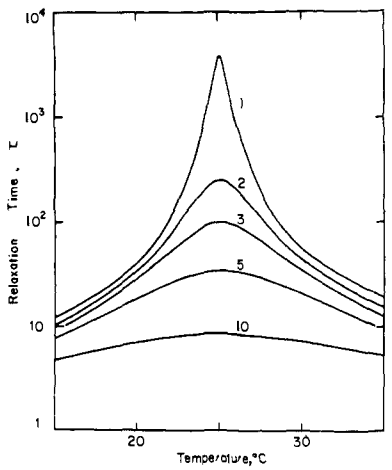

Figure 6. The relaxation times vs. temperature calculated for the simple cluster reaction scheme of eq 30 with $l_{max} = 300$. The numbers are given in ascending order of the corresponding eigenvalues. The largest relaxation time τ, reflecting the slow nucleation process shows the largest enhancement at the midpoint of the transition. The parameters used are $\epsilon = 3$ kcal/mol, $s_0\gamma = 3$ kcal/mol, $s_0\omega = 9.6$ eu, $T_m' = 25$ °C, and $\bar{b} = 1$.

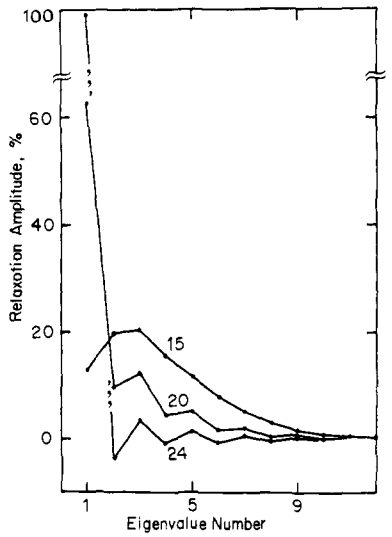

Figure 7. The relaxation amplitudes corresponding to each relaxation time calculated for the simple cluster reaction scheme of eq 30 with $l_{max} = 50$. The numbers denote temperatures. The slowest relaxation process becomes more and more predominant as the transition temperature becomes closer. The parameters used are $\epsilon = 3$ kcal/mol, $s_0\gamma = 3.4$ kcal/mol, $s_0 = 9.6$ eu, $T_m' = 25$ °C, and $\bar{b} = 1$.

rhenius activation energy. This is equivalent to the incorporation of the linearly decreasing baseline in Figure 6.

The observed values of two relaxation times for DMPC were 2.4 s and 34 ms at $T_m = 24.2$ °C, 0.5 s and 17 ms at 23.3 °C, and 0.08 s and 1.4 ms at 24.8 °C.[11] It is interesting to note that the slowest relaxation time for the lipid phase transition is about 0.1–1 s, which is to be compared with the overall protein unfolding of 1–10 s. The slow relaxation time was smaller for DPPC and the enhancement at the midpoint of the transition was also smaller.[11] These are inconsistent with the lower cooperativity of DPPC than DMPC as can be seen in Table I.

VI. Discussion

Thus far we have discussed the thermodynamic, kinetic, and some functional properties of the lipid bilayers in terms of the cluster model. The lipid phase transition has been treated as a phase separation of solidlike S and fluidlike F states. As we have stressed many times, the lipid system does not exhibit a strong first-order phase transition. Although the transition curve reproduced by using the parameters of Table II is quite sharp, the analysis suggests the relatively low cooperativity. The width of the specific heat curve was a few tenths of a degree in accordance with the experiment, but the average cluster size was estimated to be small. The ordered structure of one phase cannot extend very far because of this weak cooperativity. The coexistence of many small clusters of two phases gives rise to a high amount of structural disorders of the lipid membrane. Such disorders would facilitate the "background transport" or increase the leakiness of the lipid membrane.

Actual cell membranes are by no means the uniform system in contrast with the pure lipid membrane. But we suppose that the coexistence of many small clusters observed around the lipid phase transition temperature would be similar to what is actually taken in cell membranes. The same or similar kinds of lipids and other components would tend to segregate or form clusters. The lipid matrix described in the fluid mosaic model by Singer and Nicolson[51] may not be a uniform system because there is considerable evidence that many molecules are distributed nonrandomly in membranes.[52] The clustering of lipids would be of great biological relevance since the structural disorders can provide suitable environment for the protein conformational changes.

Although the cluster model does not intend to provide detailed information about the molecular nature of the lipid phase transition, it reveals new aspects of the "synergetic" [20] mechanism which was not the main concern of other existing models.[1-9] If one regards the lipid system as a low cooperative system, the leakiness of the lipid membrane is more suitably understood in terms of this simplified model. The significance of the low cooperativity on the kinetic behavior is not clear, but it would be essential that the lipid phase change occur faster than the protein conformational changes in order to provide suitable environment. Although we have discussed the cooperativity of the lipid phase transition in terms of the average cluster size, the starting quantity is the cluster distribution function, eq 10, which is well defined up to the critical point. The variance can also be calculated as the second moment of the distribution function.

This phenomenological model can further be applied to the behavior of the lipid system as a whole through the convenient analysis of experimental results. For example, the addition of small molecules like cholesterol or anesthetics to pure lipid systems may be interpreted in terms of the change of the parameters ϵ and γ. One of the most important and interesting extensions of the cluster model is the phase separation of binary mixtures of lipids, in which situation an Ising spin must be interpreted to represent the occupation of the lattice site by either of two lipid components. However, the interaction with membrane proteins, the other major component of biological membranes, is beyond the scope of the present treatment.

The nature of the pretransition prior to the sharp chain-melting transition in pure lipid systems is not yet well established. In order to perform a phenomenological description of the pretransition, two interesting features must be incorporated. One is the disappearance of the pretransition for small single-bilayer vesicles and the other is the hysteresis or the different transition curves for heating and cooling processes.[31] In this connection the interaction between layers and the movement of lipid molecules may require consideration. Since lipid molecules are though to be highly mobile in the plane of the bilayer, the lipid system would show both order-disorder and displacive transitions.

Acknowledgment. We wish to thank Dr. Douglas Poland for helpful criticisms and clarifying suggestions. We are also grateful to Drs. Kazuhiko Kinosita and Elliot Elson for interesting discussions. This work was supported by NSF Grant BMS 75-08690 and NIH Grant HL 18048.

References and Notes

(1) J. E. Rothman, *J. Theor. Biol.*, **38**, 1–16 (1973).
(2) S. Marcelja, *Nature (London)*, **241**, 451–453 (1973); S. Marcelja, *Biochim. Biophys. Acta*, **367**, 165–176 (1974).
(3) J. F. Nagle, *J. Chem. Phys.*, **58**, 252–264 (1973); **63**, 1255–1261 (1975); *J. Membr. Biol.*, **27**, 233–250 (1976).
(4) H. L. Scott, Jr., *J. Theor. Biol.*, **46**, 241–253 (1974); *J. Chem. Phys.*, **62**, 1347–1353 (1975); *Biochim. Biophys. Acta*, **406**, 329–346 (1975).
(5) P. Bothorel, J. Bell, and B. Lemaire, *Chem. Phys. Lipids*, **12**, 96–116 (1974); P. Bothorel, *J. Chim. Phys. Phys.-Chim. Biol.*, **71**, 1133–1141 (1974).
(6) D. Marsh, *J. Membr. Biol.*, **18**, 145–162 (1974).
(7) R. E. Jacobs, B. Hudson, and C. Andersen, *Proc. Natl. Acad. Sci. U.S.A.*, **72**, 3993–3997 (1975).
(8) J. A. McCammon and J. M. Deutch, *J. Am. Chem. Soc.*, **97**, 6675–6681 (1975).
(9) M. B. Jackson, *Biochemistry*, **15**, 2555–2561 (1976).
(10) H.-J. Hinz and J. M. Sturtevant, *J. Biol. Chem.*, **247**, 6071–6075 (1972); S. Mabrey and J. M. Sturtevant, *Proc. Natl. Acad. Sci. U.S.A.*, **73**, 3862–3866 (1976).
(11) T. Y. Tsong, *Proc. Natl. Acad. Sci. U.S.A.*, **71**, 2684–2688 (1974); T. Y. Tsong and M. I. Kanehisa, *Biochemistry*, **16**, 2674–268 (1977).
(12) D. Papahadjopoulos, K. Jacobson, S. Nir, and T. Isac, *Biochim. Biophys. Acta*, **311**, 330–348 (1973).
(13) M. C. Blok, E. C. M. van der Neut-Kok, L. L. M. van Deenen, and J. De Gier, *Biochim. Biophys. Acta*, **406**, 187–196 (1975).
(14) T. Y. Tsong, *Biochemistry*, **14**, 5409–5414 (1975); T. Y. Tsong, M. Greenberg, and M. I. Kanehisa, *ibid.*, **16**, 3115–3121 (1977).
(15) D. Marsh, A. Watts, and P. F. Knowles, *Biochemistry*, **15**, 3570–3578 (1976).
(16) R. Lawaczeck, M. Kainosho, J.-L. Girardet, and S. I. Chan, *Nature (London)*, **256**, 584–586 (1975).
(17) C. D. Linden, K. L. Wright, H. M. McConnell, and C. F. Fox, *Proc. Natl. Acad. Sci. U.S.A.*, **70**, 2271–2275 (1973).
(18) S. H. Wu and H. M. McConnell, *Biochem. Biophys. Res. Commun.*, **55**, 484–491 (1973).
(19) J. A. F. Op den Kamp, J. De Gier, and L. L. M. van Deenen, *Biochim. Biophys. Acta*, **345**, 253–256 (1974); J. A. F. Op den Kamp, M. T. Kauerz, and L. L. M. van Deenen, *Ibid.*, **406**, 169–177 (1975).
(20) G. Adam, *Z. Naturforsch. B*, **23**, 181–197 (1968); G. Adam in "Synergetics", H. Haken, Ed., B. G. Teubner, Stuttgart, 1973, pp 220–231.
(21) J.-P. Changeux, J. Thiery, Y. Tung, and C. Kittel, *Proc. Natl. Acad. Sci. U.S.A.*, **57**, 335–341 (1967); R. Blumenthal, J.-P. Changeux, and R. Lefever, *J. Membr. Biol.*, **2**, 351–374 (1970).
(22) T. L. Hill, *Proc. Natl. Acad. Sci. U.S.A.*, **58**, 111–114 (1967); T. L. Hill and Y.-D. Chen, *ibid.*, **65**, 1069–1076 (1970); Y.-D. Chen and T. L. Hill, *Ibid.*, **70**, 62–65 (1973).
(23) J. Frenkel, "Kinetic Theory of Liquids", Oxford University Press, London, 1946.
(24) M. E. Fisher, *Physics*, **3**, 255–283 (1967); M. E. Fisher, in "Proceedings of the International School of Physics (Enrico Fermi)", M. S. Green, Ed., Academic Press, New York, N.Y., 1971, pp 1–99.
(25) K. Binder and D. Stauffer, *J. Stat. Phys.*, **6**, 49–59 (1972); E. Stoll, K. Binder, and T. Schneider, *Phys. Rev. B*, **6**, 2777–2780 (1972).
(26) C. Domb in "Phase Transitions and Critical Phenomena", Vol. 3, C. Domb and M. S. Green, Ed., Academic Press, New York, N.Y., 1974, pp 357–484.
(27) H. E. Stanley, "Introduction to Phase Transitions and Critical Phenomena", Oxford University Press, London, 1971.
(28) D. Poland and H. A. Scheraga, "Theory of Helix-Coil Transitions in Biopolymers", Academic Press, New York, N.Y., 1970.
(29) A. Ikegami, *Biophys. Chem.*, **6**, 117–130 (1977); M. I. Kanehisa and A. Ikegami, *ibid.*, **6**, 131–149 (1977).
(30) C. Huang, *Biochemistry*, 8, 344–352 (1969).
(31) J. Suurkuusk, B. R. Lentz, Y. Barenholz, R. L. Biltonen, and T. E. Thompson, *Biochemistry*, **15**, 1393–1401 (1976).
(32) M. C. Phillips and D. Chapman, *Biochim. Biophys. Acta*, **163**, 301–313 (1968).
(33) B. J. Hiley and M. F. Sykes, *J. Chem. Phys.*, **34**, 1531–1537 (1961).
(34) K. Binder and D. Stauffer, *Adv. Phys.*, **25**, 343–396 (1976).
(35) K. Inoue, *Biochim. Biophys. Acta*, **339**, 390–402 (1974).
(36) P. Nicholls and N. Miller, *Biochim. Biophys. Acta*, **356**, 184–198 (1974).
(37) M. C. Blok, L. L. M. van Deenen, and J. De Gier, *Biochim. Biophys. Acta*, **433**, 1–12 (1976).
(38) M. K. Jain, "The Bimolecular Lipid Membrane: A System", Van Nostrand-Reinhold, Princeton, N.J., 1972.
(39) H. T. Tien, "Bilayer Lipid Membranes (BLM)", Marcel Dekker, New York, N.Y., 1974.
(40) D. Papahadjopoulos and H. K. Kimelberg, *Prog. Surf. Sci.*, **4**, 141–232 (1973).
(41) H. Hauser, M. C. Phillips, and M. Stubbs, *Nature (London)*, **239**, 342–344 (1972); H. Hauser, D. Oldani, and M. C. Phillips, *Biochemistry*, **12**, 4507–4517 (1973).
(42) R. Whittam, "Transport and Diffusion in Red Blood Cells", Williams and Wilkins, Baltimore, Md., 1964.
(43) T. Y. Tsong, unpublished data.
(44) V. Luzzatti, *Biol. Membr.*, 1, 71–123 (1968).
(45) H. Träuble, *Naturwissenschaften*, **58**, 277–284 (1971).
(46) K. Binder, D. Stauffer, and H. Muller-Krumbhaar, *Phys. Rev. B*, **12**, 5261–5287 (1975).
(47) B. T. Smith, J. M. Boyle, J. J. Dongarra, B. S. Garbow, Y. Ikebe, V. C. Klema, and C. B. Moler, "Matrix Eigensystem Routines—EISPACK Guide", 2nd ed, Springer-Verlag, West Berlin, 1976.
(48) E. L. Elson, *Biopolymers*, 11, 1499–1520 (1972).
(49) G. Schwarz, *J. Mol. Biol.*, 11, 64–77 (1965).
(50) By mistake two amplitudes α_1 and α_2 were interchanged in Table II of ref 11, Tsong and Kanehisa (1977).
(51) S. J. Singer and G. L. Nicolson, *Science*, **175**, 720–731 (1972).
(52) M. K. Jain and H. B. White, *Adv. Lipid Res.*, **15**, 1–60 (1977).
(53) Abbreviations: DMPC, dimyristoylphosphatidylcholine; DPPC, dipalmitoylphosphatidylcholine; DSPC, distearoylphosphotidylcholine; BLM, bilayer lipid membrane; PS, phosphotidylserine; DPPG, dipalmitoylphosphatidylglycerol; PA, phosphatidic acid; ANS, 8-anilino-1-naphthalene sulfonate; BTB, bromothymol blue.